Modelling the future health, equity, economic and global impacts of pandemic recovery actions for urban mobility

Dr. Kerry A. Nice
A. Prof Jason Thompson

Transport, Health, and Urban Design Research Lab, Melbourne School of Design
University of Melbourne

August 24, 2022

Building on:

In response to the COVID-19 pandemic, most countries implemented public health ordinances that resulted in restricted mobility and a resultant change in air quality. This has provided an opportunity to quantify the extent to which carbon-based transport and industrial activity affect air quality. In this study, confounding factors were disentangled for a direct comparison of pandemic-related reductions in absolute pollutions levels, globally. The non-linear relationships between atmospheric processes and daily ground-level NO_2, PM_{10}, $PM_{2.5}$ and O_3 measurements were captured in city- and pollutant-specific XGBoost models for over 700 cities, adjusting for weather, seasonality and trends. City-level modelling allowed adaptation to the distinct topography, urban morphology, climate and atmospheric conditions for each city, individually, as the weather variables that were most predictive varied across cities. Pollution forecasts for 2020 in absence of a pandemic were generated based on weather and formed an ensemble for country-level pollution reductions. Findings were robust to modelling assumptions and consistent with various published case studies. NO2 reduced most in China, Europe and India, following severe government restrictions as part of the initial lockdowns. Reductions were highly correlated with changes in mobility levels, especially trips to transit stations, workplaces, retail and recreation venues. Further, NO_2 did not fully revert to pre-pandemic levels in 2020. Ambient $PM_{2.5}$ pollution, which has severe adverse health consequences, reduced most in China and India. Increased O_3 levels during initial lockdowns have been documented widely. However, our analyses found a subsequent reduction in O_3 for many countries below what was expected based on meteorological conditions during summer months (e.g., China, United Kingdom, France, Germany, Poland, Turkey). The effects in periods with high O_3 levels are especially important for the development of effective mitigation strategies to improve health outcomes.

Wijnands, Jasper S., Nice, Kerry A., Seneviratne, Sachith, Thompson, Jason and Stevenson, Mark (2022) The impact of the COVID-19 pandemic on air pollution: A global assessment using machine learning techniques, Atmospheric Pollution Research, 13(6), p. 101438. doi: 10.1016/j.apr.2022.101438.

Pollution modelling process overview

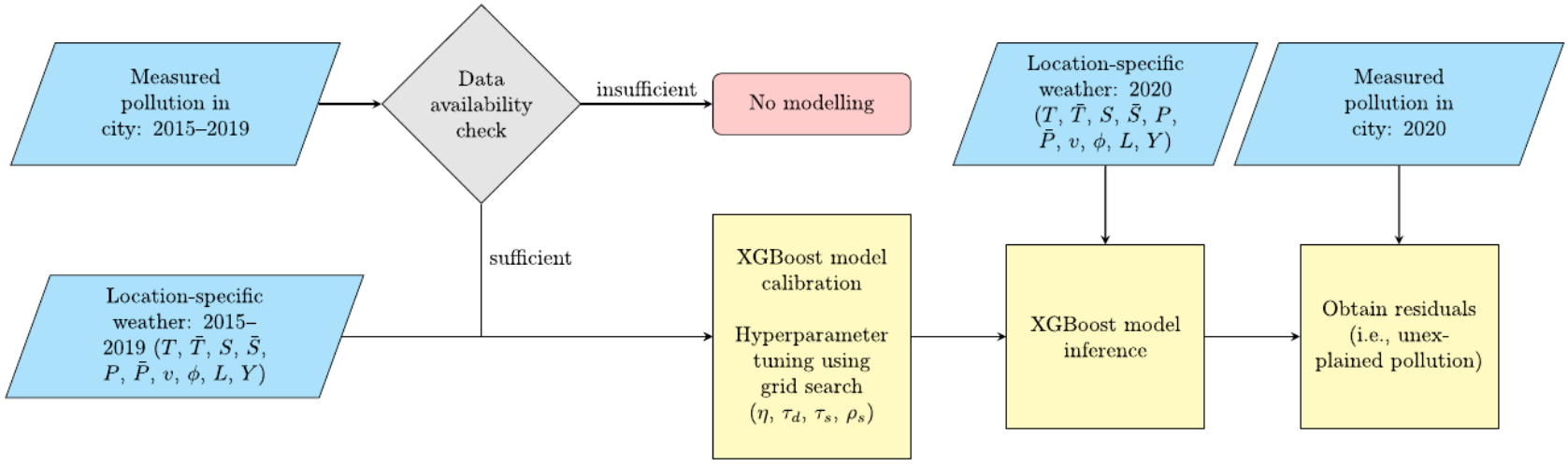

Combining ERA5 weather data with ground level pollution data, creating pollutant and city specific XGBoost model for 700 cities. Calculate 2020 pollution anomalies in the absence of the COVID-19 pandemic.

Data sources: Weather and ground level pollution

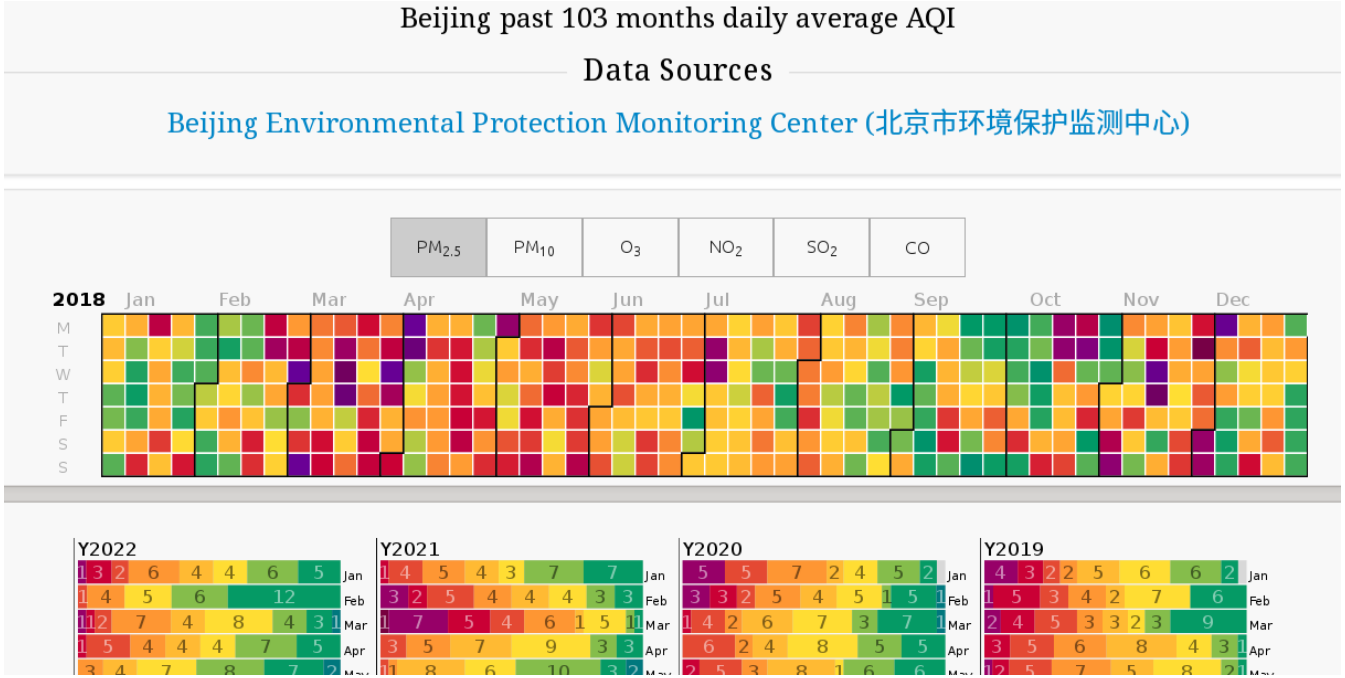

Daily ground level NO_2, PM_{10}, $PM_{2.5}$ and O_3 for 132 countries from AQICN.

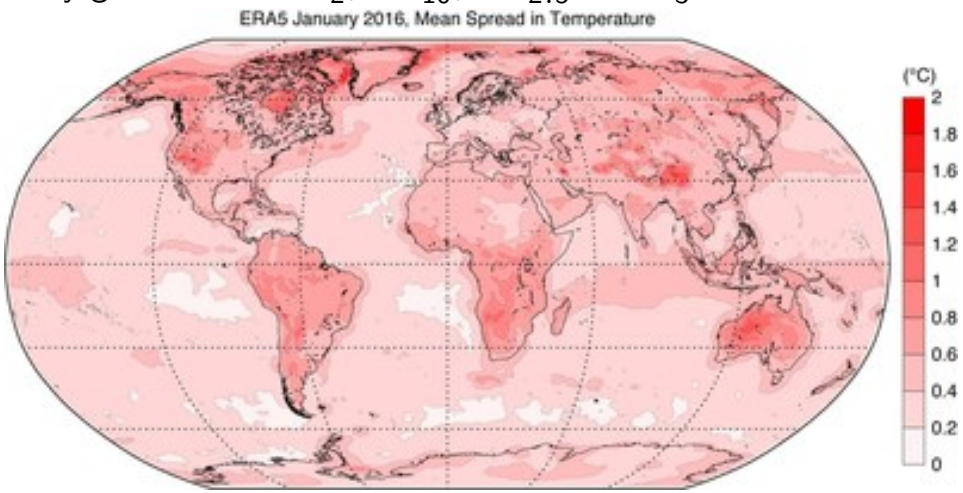

Hourly ERA5 weather (2m air temperature, net solar radiation, total precipitation, mean wind speed, mean wind direction, mean leaf area index). 2015-2019 for model training, 2020 for validation and analysis.

XGBoost hyperparameter tuning, selected features for XGBoost models

Grid search to tune XGBoost hyperparameters that influence its learning process (number and length of decision trees, samples required for single node, etc).

Table 1
Initial and reduced hyperparameter sets for grid search.

Hyperparameter	Initial set	Final set
η	{0.01, 0.05, 0.10}	{0.01, 0.05}
τ_d	{2, 4, 5, 6, 8, 10}	{5, 6, 8}
τ_s	{1, 3, 5, 7}	{5, 7}
ρ_s	{0.5, 0.6, 0.7, 0.8, 1}	{0.5, 0.6}
ρ_f	{0.8, 1}	{1}

Final selection of features included in XGBoost models, including air temperature on day, mean air temperature of previous 3 days, total precipitation on day and sum of previous 3 days, etc. Note, day of week not included to allow later mobility reduction analysis.

Table 2
Selected features for XGBoost models.

Variable	Description
T	Air temperature at 2 m altitude, day t
$\bar{T}$	Air temperature at 2 m altitude, mean of days t–3, t–2, t–1
S	Net solar radiation at the surface, day t
$\bar{S}$	Net solar radiation at the surface, mean of days t–3, t–2, t–1
P	Total precipitation, day t
$\bar{P}$	Total precipitation, sum of days t–3, t–2, t–1
v	Wind speed, day t
ϕ	Wind direction, day t
L	Leaf area index of vegetation, day t
Y	Year of observation

Calibrated models for individual cities and pollutants that incorporate weather patterns, pollution seasonal trends, and long term pollution trends. Can predict 2020 pollution levels (in absence of pandemic).

2020 forecast pollution vs actual

Actual (black) and forecasted (blue) pollution levels

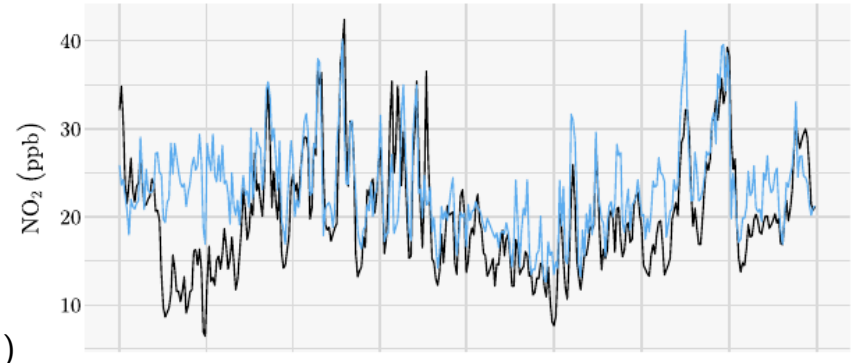

a) NO_2 in Chongqing

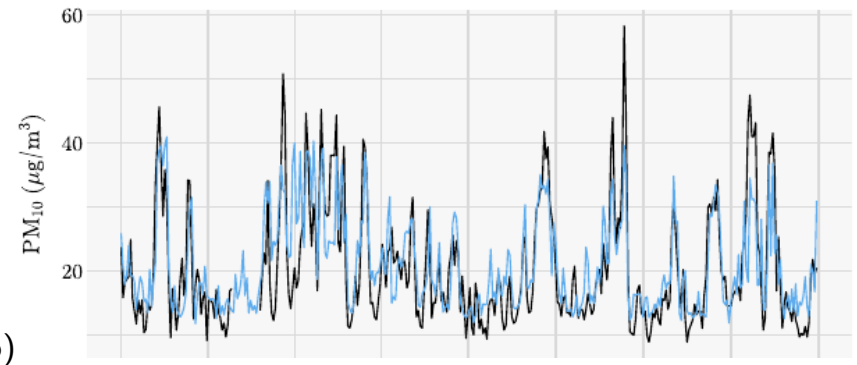

b) PM_{10} in Antwerpen, Belgium

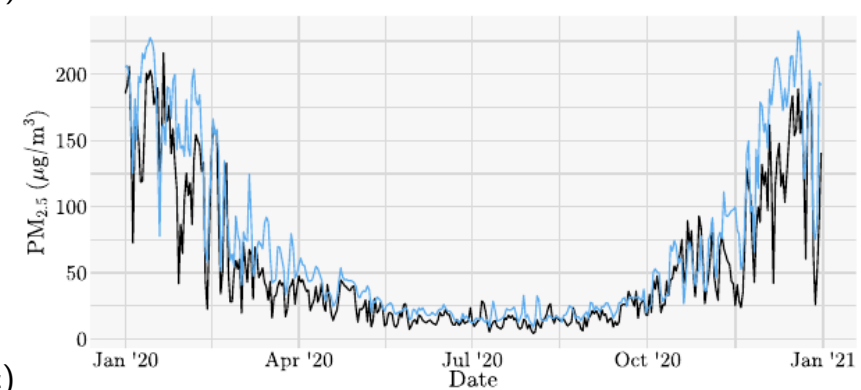

c) $PM_{2.5}$ in Ulaanbaatar, Mongolia

- Large February NO_2 reductions in China resulting from lockdowns.
- Aug 2020 Belgium heatwave accurately reflected through increased PM_{10} levels.
- Temperature influence on pollution: seasonal trends of $PM_{2.5}$ in Mongolia from winter heating.

Unexplained NO_2, $PM_{2.5}$, and O_3 across cities, stringency of COVID-19 restrictions, and mobility patterns from Google mobility data.

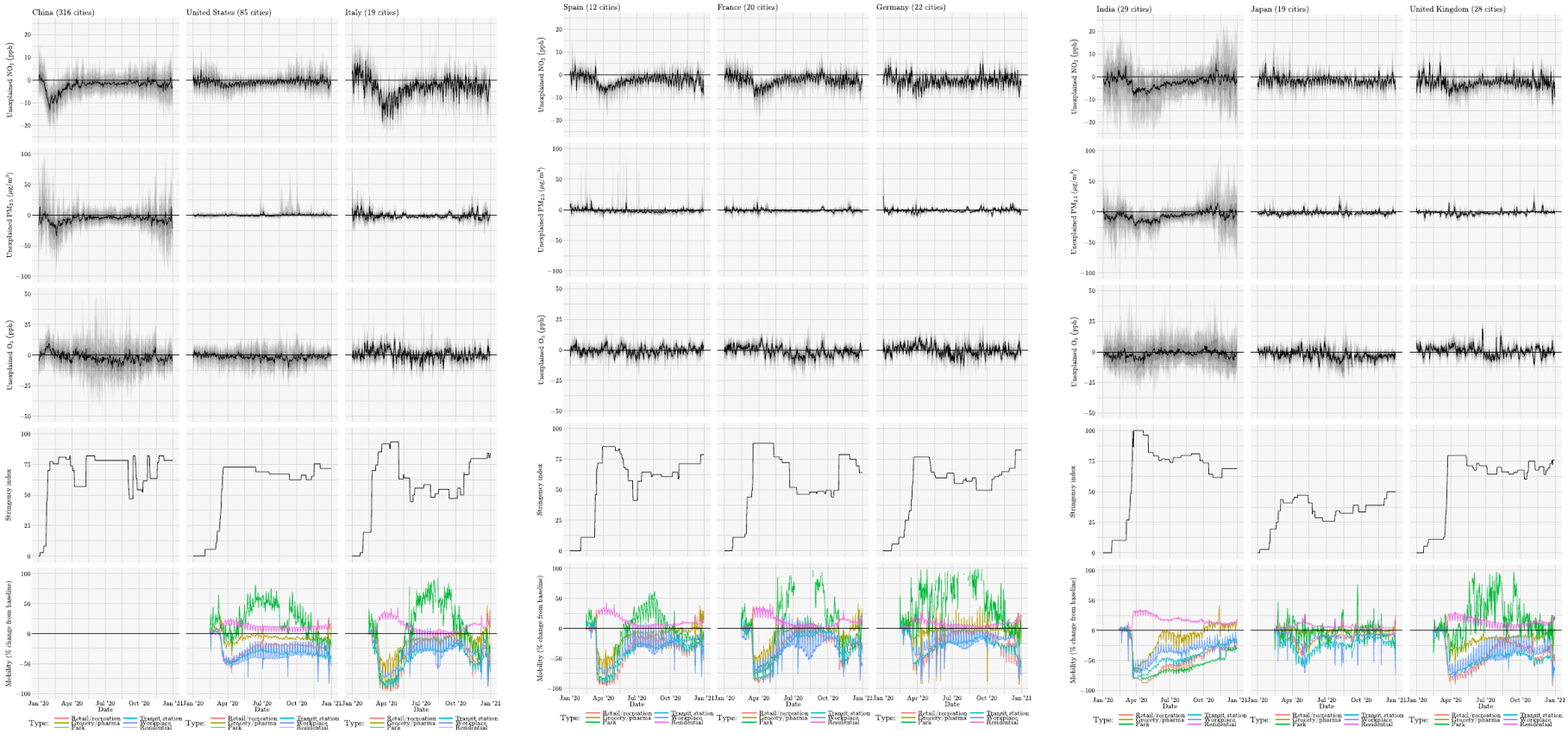

Large reductions in NO_2 in most places across the first few months of 2020, largely returning to normal levels afterwards. $PM_{2.5}$ reductions in many places across 2020. O_3 increases in the first half of 2020 (due to NO_2 reductions) but below normal levels mid-year.

Correlations between mobility and unexplained NO_2, computed per country from mid-February to mid-April

Country	Maximum stringency	n	Transit stations	Workplaces	Retail and recreation	Grocery and pharmacy	Parks	Residential
Croatia	96.3	46	0.98	0.97	0.98	0.94	0.91	-0.97
Colombia	88.0	61	0.97	0.97	0.97	0.94	0.97	-0.97
Serbia	100.0	61	0.96	0.96	0.95	0.94	0.92	-0.96
Denmark	72.2	61	0.92	0.91	0.92	0.84	-0.60	-0.92
Bosnia and Herzegovina	92.6	61	0.90	0.89	0.88	0.84	0.83	-0.90
Israel	94.4	177	0.86	0.82	0.82	0.80	0.75	-0.84
Finland	67.6	122	0.80	0.78	0.76	0.80	-0.48	-0.81
Bolivia	84.3	36	0.78	0.78	0.79	0.78	0.77	-0.78
Indonesia	71.8	61	0.72	0.79	0.78	0.74	0.72	-0.81
Spain	85.2	693	0.76	0.77	0.75	0.73	0.74	-0.80
Romania	87.0	183	0.77	0.76	0.76	0.74	0.75	-0.77
Hungary	76.9	61	0.73	0.75	0.74	0.84	0.77	-0.75
Belgium	81.5	60	0.76	0.73	0.76	0.74	0.57	-0.75
Austria	81.5	61	0.73	0.72	0.72	0.69	0.73	-0.73
Portugal	88.0	122	0.68	0.71	0.68	0.74	0.67	-0.70
France	88.0	1213	0.70	0.72	0.69	0.68	0.69	-0.72
New Zealand	96.3	122	0.69	0.69	0.72	0.74	0.66	-0.66
Switzerland	73.2	181	0.73	0.64	0.71	0.66	0.21	-0.68
Italy	93.5	1085	0.66	0.70	0.67	0.69	0.66	-0.71
Czech Republic	82.4	94	0.59	0.60	0.55	0.64	0.25	-0.58
China	81.9	427	0.45	0.59	0.51	0.70	0.29	-0.69
Brazil	74.5	329	0.61	0.62	0.57	0.51	0.63	-0.62
Germany	76.9	1303	0.54	0.57	0.58	0.65	-0.06	-0.57
Ireland	90.7	28	0.56	0.58	0.59	0.59	0.57	-0.57
Estonia	77.8	61	0.61	0.52	0.59	0.57	0.49	-0.59
South Africa	88.0	271	0.57	0.58	0.55	0.51	0.49	-0.58
Vietnam	96.3	108	0.66	0.46	0.57	0.67	0.79	-0.42
United Kingdom	79.6	1387	0.57	0.58	0.55	0.48	0.37	-0.59
Norway	79.6	61	0.56	0.57	0.57	0.48	-0.34	-0.55
Poland	83.3	488	0.50	0.56	0.49	0.54	0.49	-0.52
Bulgaria	73.2	105	0.46	0.41	0.41	0.28	0.31	-0.40
Mongolia	65.7	61	0.42	0.23	0.46	0.32	0.20	-0.35
United States	72.7	3961	0.34	0.36	0.37	0.20	0.02	-0.37
India	100.0	1594	0.30	0.32	0.30	0.32	0.29	-0.33
Argentina	100.0	94	0.32	0.28	0.30	0.35	0.30	-0.30
Chile	73.2	183	0.34	0.34	0.27	0.17	0.15	-0.37
North Macedonia	–	61	0.25	0.30	0.25	0.31	0.11	-0.24
Japan	45.4	1038	0.41	0.29	0.34	-0.06	-0.06	-0.35
Canada	74.5	755	0.29	0.25	0.27	0.19	0.22	-0.27
Netherlands	79.6	305	0.22	0.24	0.30	0.19	0.14	-0.26
Mexico	82.4	781	0.16	0.16	0.18	0.27	0.21	-0.14
Thailand	76.9	549	0.16	0.16	0.17	0.15	0.17	-0.17
Turkey	77.8	774	0.22	0.12	0.10	0.07	0.15	-0.10
Slovakia	87.0	61	0.09	0.11	0.11	0.15	0.30	-0.10
Sweden	64.8	122	0.08	0.06	0.02	0.03	0.04	-0.06
South Korea	82.4	1464	-0.05	0.21	-0.03	-0.42	-0.42	-0.07

Many countries show high correlations between journeys to workplaces and NO_2 reductions.

Robustness of results, comparison to other modelling approaches

Actual (black), XGBoost (blue), linear regression (red), Gamma GLM (orange), random forest (light blue) and time series (green) forecasts across 2020.
(a) NO_2 in Urumqi, China; (b) NO_2 in Santiago, Chile; and (c) PM_{10} in Pune, India.

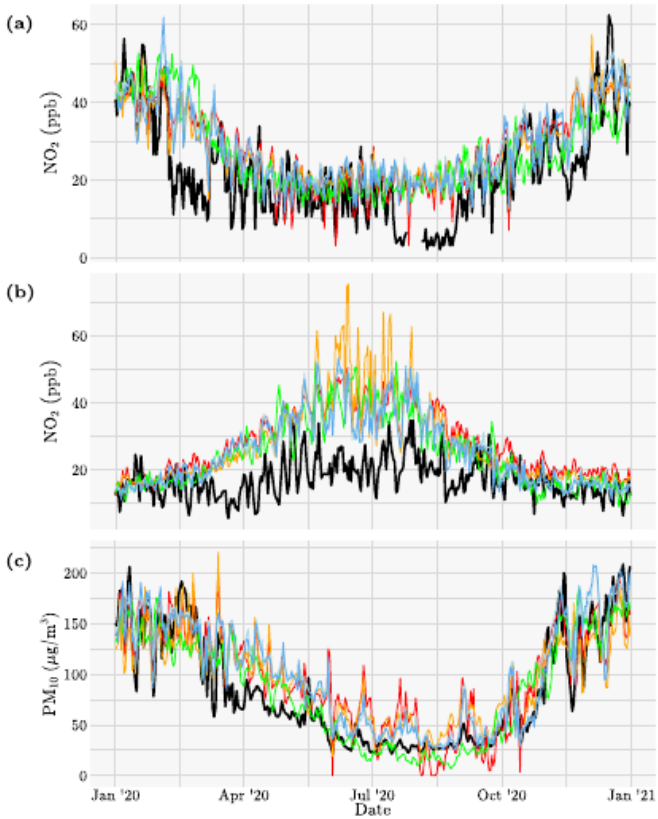

MAE of forecasts during the first two weeks of January 2020, for different modelling approaches.

	Time series	Linear model	Gamma GLM	Random forest	XGBoost
NO_2 (ppb)	5.45	5.01	5.19	4.40	4.18
PM_{10} (μg/m³)	28.02	21.76	21.78	21.78	21.09
$PM_{2.5}$ (μg/m³)	20.01	16.69	17.96	16.58	16.68
O_3 (ppb)	6.68	7.52	8.20	6.05	6.28

RMSE of forecasts during the first two weeks of January 2020, for different modelling approaches.

	Time series	Linear model	Gamma GLM	Random forest	XGBoost
NO_2 (ppb)	6.54	5.95	6.47	5.37	5.13
PM_{10} (μg/m³)	34.07	26.81	27.89	26.50	26.18
$PM_{2.5}$ (μg/m³)	24.44	21.20	24.09	20.65	21.02
O_3 (ppb)	8.08	8.93	9.72	7.37	7.60

All methods captured seasonal pollution patterns of cities.
XGBoost generally obtained best out-of-sample performance compared to other modelling approaches.

Comparison of results to other studies that quantified air pollution changes in 2020

Adams (2020)	Ontario, Canada	22-Mar–25-Apr	NO_2	−2 ppb	−1.9 ppb
Adams (2020)	Ontario, Canada	22-Mar–25-Apr	$PM_{2.5}$	0 $\mu g/m^3$	−0.6 $\mu g/m^3$
Adams (2020)	Ontario, Canada	22-Mar–25-Apr	O_3	−1 ppb	1.1 ppb
Archer et al. (2020)	United States	1-Apr–30-Apr	NO_2	−2.02, −1.3 ppb[a]	−2.5 ppb
Archer et al. (2020)	United States	1-Apr–30-Apr	$PM_{2.5}$	0.05, 0.28 $\mu g/m^3$[a]	−0.1 $\mu g/m^3$
Berman and Ebisu (2020)	United States	8-Jan–12-Mar	NO_2	−1.17 ppb	−0.6 ppb
Berman and Ebisu (2020)	United States	13-Mar–21-Apr	NO_2	−4.76 ppb	−2.9 ppb
Berman and Ebisu (2020)	United States	8-Jan–12-Mar	$PM_{2.5}$	−0.29 $\mu g/m^3$	−0.6 $\mu g/m^3$
Berman and Ebisu (2020)	United States	13-Mar–21-Apr	$PM_{2.5}$	−0.28 $\mu g/m^3$	−0.1 $\mu g/m^3$
Connerton et al. (2020)	Los Angeles, USA	1-Mar–31-Mar	$PM_{2.5}$	−2.99 $\mu g/m^3$	−1.9 $\mu g/m^3$
Connerton et al. (2020)	New York, USA	1-Mar–31-Mar	$PM_{2.5}$	−2.03 $\mu g/m^3$	−4.5 $\mu g/m^3$
Connerton et al. (2020)	Paris, France	1-Mar–31-Mar	$PM_{2.5}$	−2.56 $\mu g/m^3$	−2.4 $\mu g/m^3$
Connerton et al. (2020)	São Paulo, Brazil	1-Mar–31-Mar	$PM_{2.5}$	−0.54 $\mu g/m^3$	−0.3 $\mu g/m^3$
Jia et al. (2020)	Memphis, USA	25-Mar–4-May	$PM_{2.5}$	0.3 $\mu g/m^3$	0.1 $\mu g/m^3$
Jia et al. (2020)	Memphis, USA	25-Mar–4-May	O_3	−1.9 ppb	−1.6 ppb
Ordóñez et al. (2020)	Europe	15-Mar–30-Apr	NO_2	−9.2, −13.1 $\mu g/m^3$[b]	−10.7 $\mu g/m^3$
Ordóñez et al. (2020)	Europe	15-Mar–30-Apr	O_3	6.2, 0.1 $\mu g/m^3$[b]	4.5 $\mu g/m^3$
Petetin et al. (2020)	Spain	14-Mar–29-Mar	NO_2	−3.4, −5.6 ppb[c]	−5.9 ppb
Petetin et al. (2020)	Spain	30-Mar–9-Apr	NO_2	−5.2, −7.4 ppb[c]	−6.8 ppb
Petetin et al. (2020)	Spain	10-Apr–23-Apr	NO_2	−4.3, −6.8 ppb[c]	−6.1 ppb
Ropkins and Tate (2021)	United Kingdom	10-Mar–10-Apr	NO_2	−4.16, −7.58 $\mu g/m^3$[d]	−8.1 $\mu g/m^3$
Ropkins and Tate (2021)	United Kingdom	10-Mar–10-Apr	$PM_{2.5}$	4.79, 5 $\mu g/m^3$[d]	−1.7 $\mu g/m^3$
Ropkins and Tate (2021)	United Kingdom	10-Mar–10-Apr	O_3	6.96, 7.39 $\mu g/m^3$[d]	5.8 $\mu g/m^3$
Tanzer-Gruener et al. (2020)	Pittsburgh, USA	14-Mar–30-Apr	$PM_{2.5}$	−2.8 $\mu g/m^3$	−1.7 $\mu g/m^3$
Venter et al. (2020)	China	24-Jan–15-May	$PM_{2.5}$	−16 $\mu g/m^3$	−9.2 $\mu g/m^3$
Venter et al. (2020)	India	29-Feb–15-May	$PM_{2.5}$	−15 $\mu g/m^3$	−15.6 $\mu g/m^3$
Zheng et al. (2020)	Wuhan, China	23-Jan–22-Feb	$PM_{2.5}$	−24.8 $\mu g/m^3$	−28.9 $\mu g/m^3$

Global anomalies: $PM_{2.5}$ on 9 February 2020

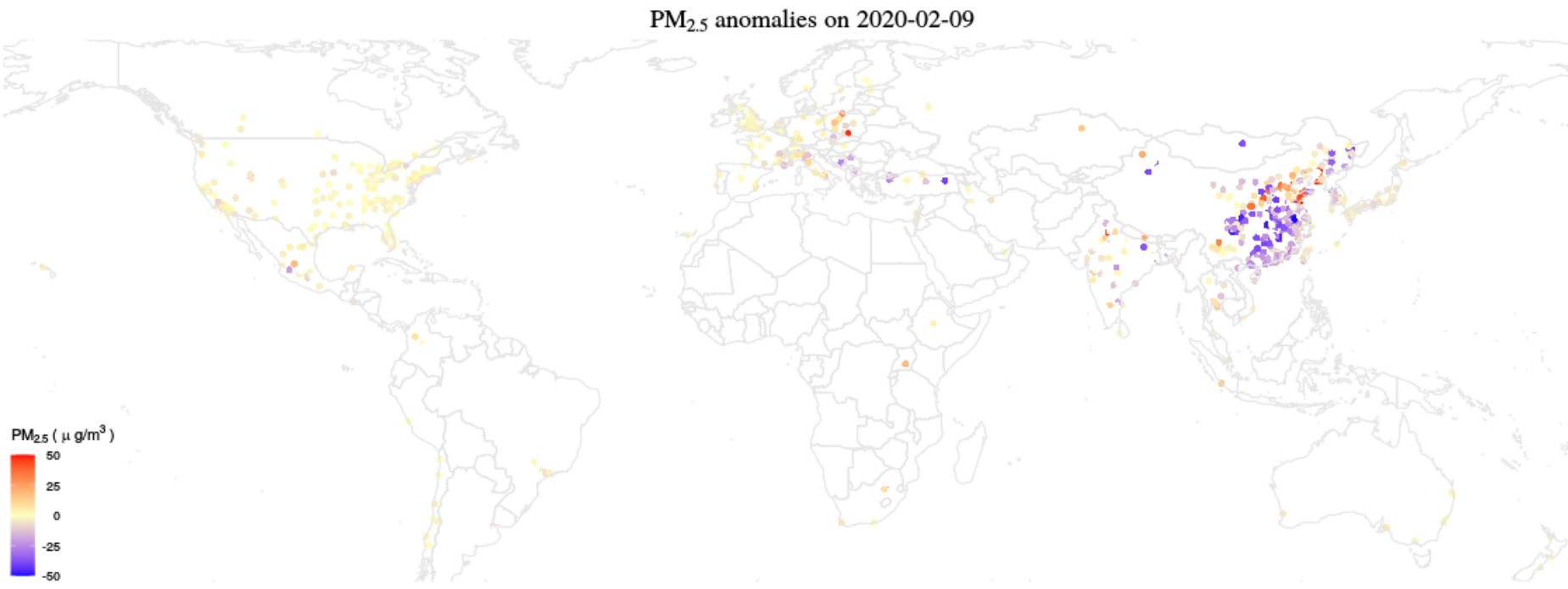

Reductions of $PM_{2.5}$ in China

Global anomalies: NO_2 on 4 April 2020

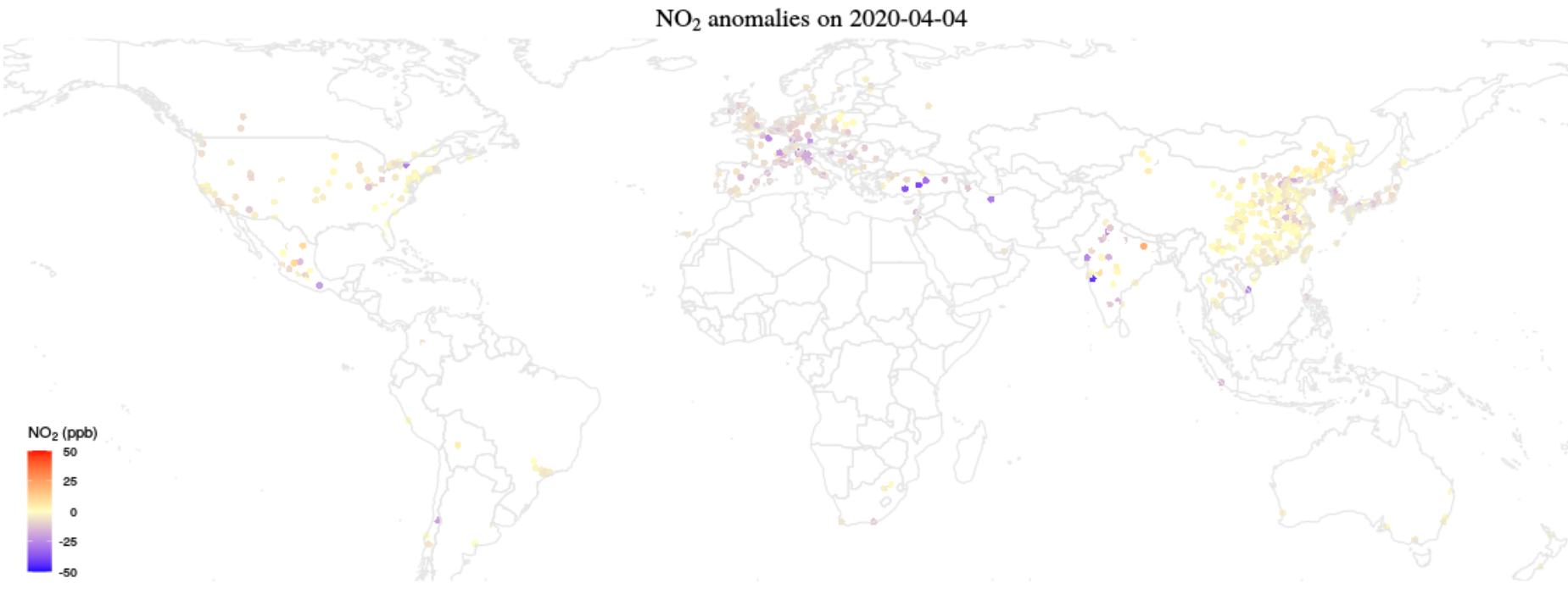

Reductions of NO_2 in Europe

Global anomalies: O_3 on 30 January 2020

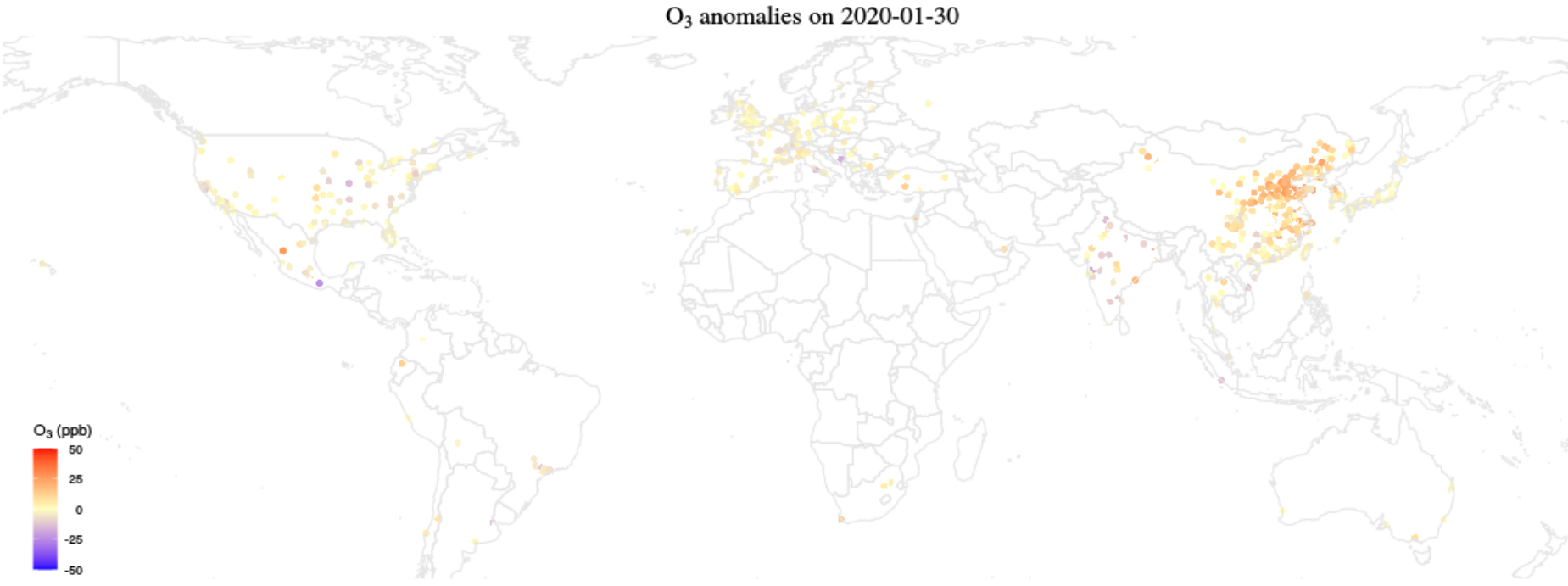

Increases of O_3 in China.

Unexamined questions

Figure 4. Stringency Index and daily cases per 100,000 for 50 states and DC to December 1 (sources: OxCGRT and JHU)[8]

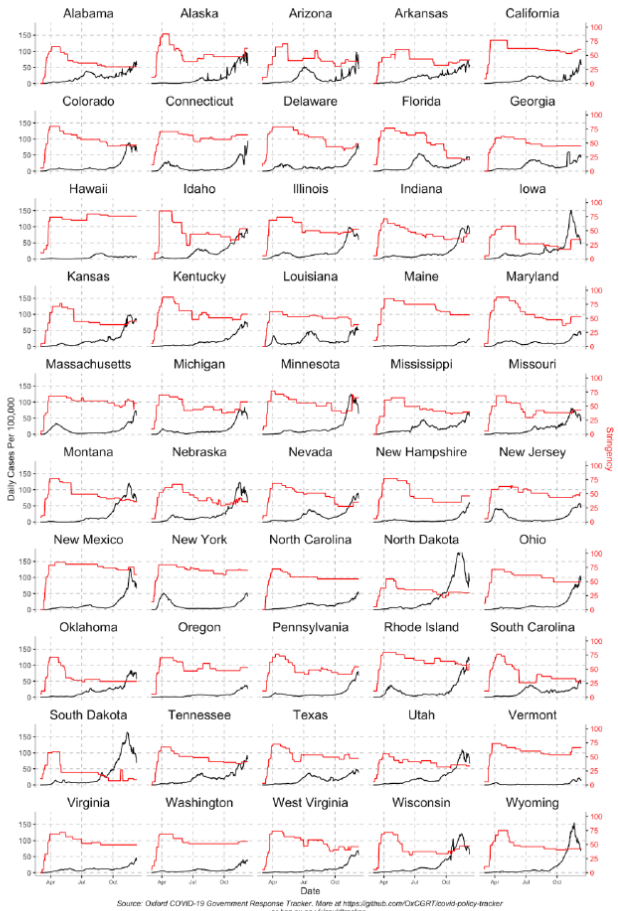

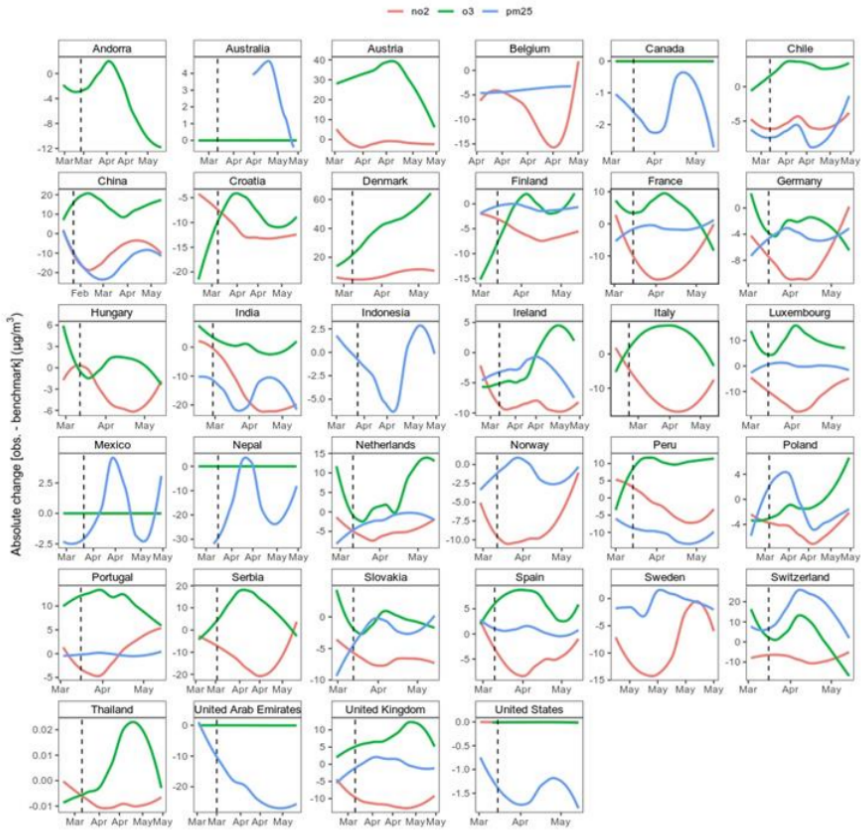

Fig. S5. Ground-level pollutant time series and lockdown dates. Daily time series of ground-level NO_2, O_3 and $PM_{2.5}$ anomalies (observed subtract benchmark model predicted values) per country with dates of lockdown indicated by vertical lines. Smoothed loess regression lines are fitted to indicate moving averages. Lines for each pollutant are plotted on the same Y-axis and thus pollutants with very small temporal variation from the benchmark appear flat (e.g. O_3 for Australia). Please consult interactive web application for individual plots: https://nina.earthengine.app/view/lockdown-pollution

Pollution anomalies varied globally under different stringencies and differing transport systems.

Unexamined questions

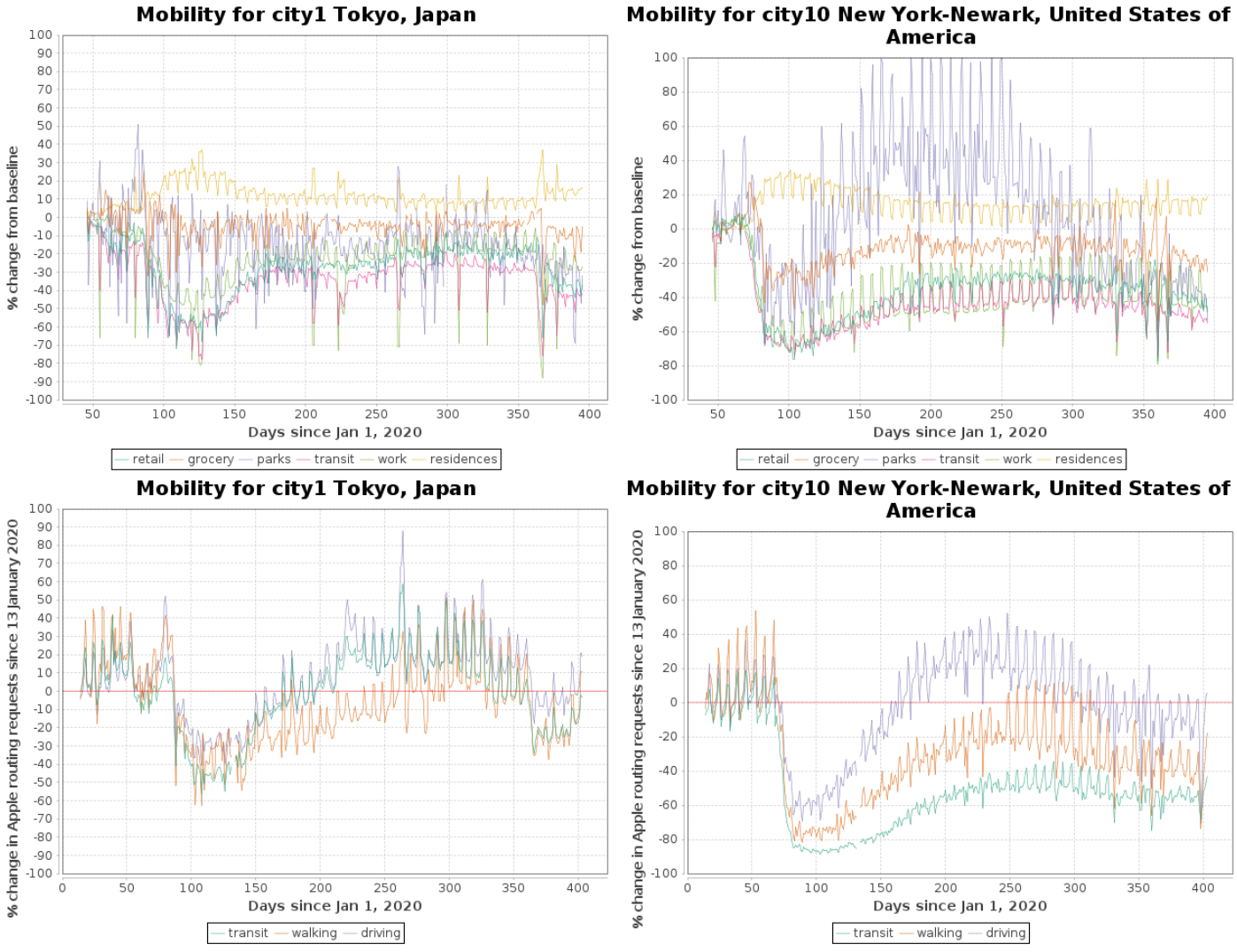

How do pollution levels vary in different cities with different mobility profiles? (Top) Google mobility showing locations, (bottom) Apple mobility showing transport mode map requests.

Lancet clusters vs NO2 anomalies, Jan-Jun 2020

Lancet clusters vs O3 anomalies, Jan-Jun 2020

Lancet clusters vs PM10 anomalies, Jan-Jun 2020

Lancet clusters vs PM2.5 anomalies, Jan-Jun 2020

Paper proposal

What urban design characteristics did each city have to work with?

What limitations and affordances did these features offer them?

Which cities demonstrated the optimal combination of outcomes across Mobility (e.g., economic activity), mode choice (e.g., pollution and risk exposure), and infectious disease outcomes at time t?

Build on 2-dimensional understanding of trade-off between mobility / liberties and outcomes from Oliu-Barton, M., et al. (2021). "SARS-CoV-2 elimination, not mitigation, creates best outcomes for health, the economy, and civil liberties." The Lancet **397**(10291): 2234-2236.